One pot Hydrothermal synthesis of Molybdenum Nickel Sulfide with GQDs as a novel conductive additive for enhanced supercapacitive performance

Omkar Sangabathula* and Chandra S. Sharma

Creative & Advanced Research Based On Nanomaterials (CARBON) Laboratory,

Department of Chemical Engineering, Indian Institute of Technology Hyderabad,

Kandi, 502285, Sangareddy, Telangana, India

*Corresponding author: Email: ch18resch01007@iith.ac.in

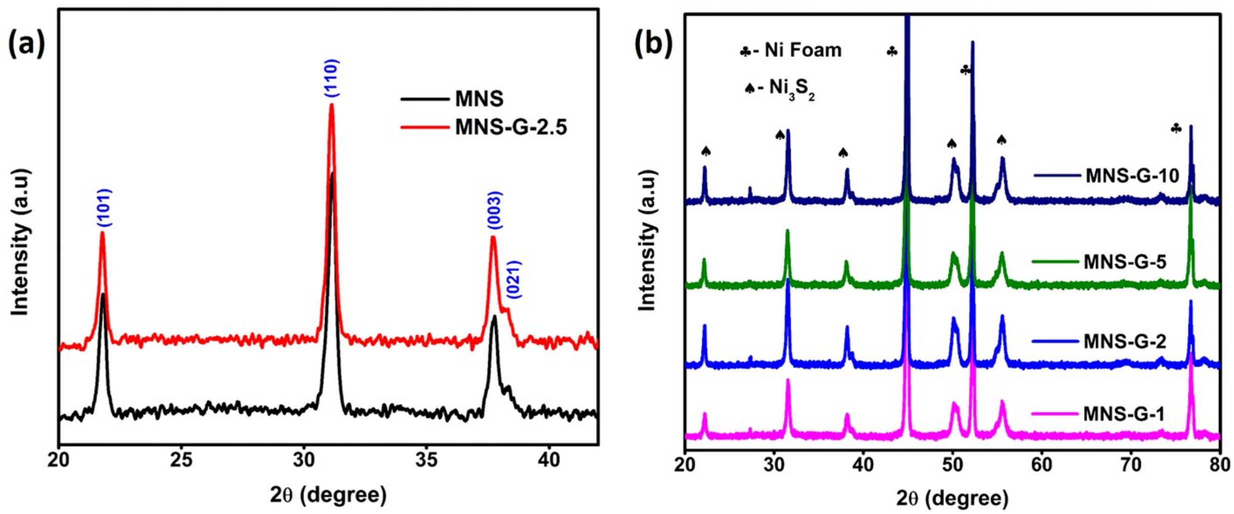

Figure S1. (a) The enlarged view of the XRD pattern of MNS and MNS-G-2.5 composites prepared on nickel foam (b) XRD patterns of MNS-G-1, MNS-G-2, MNS-G-5 and MNS-G-10.

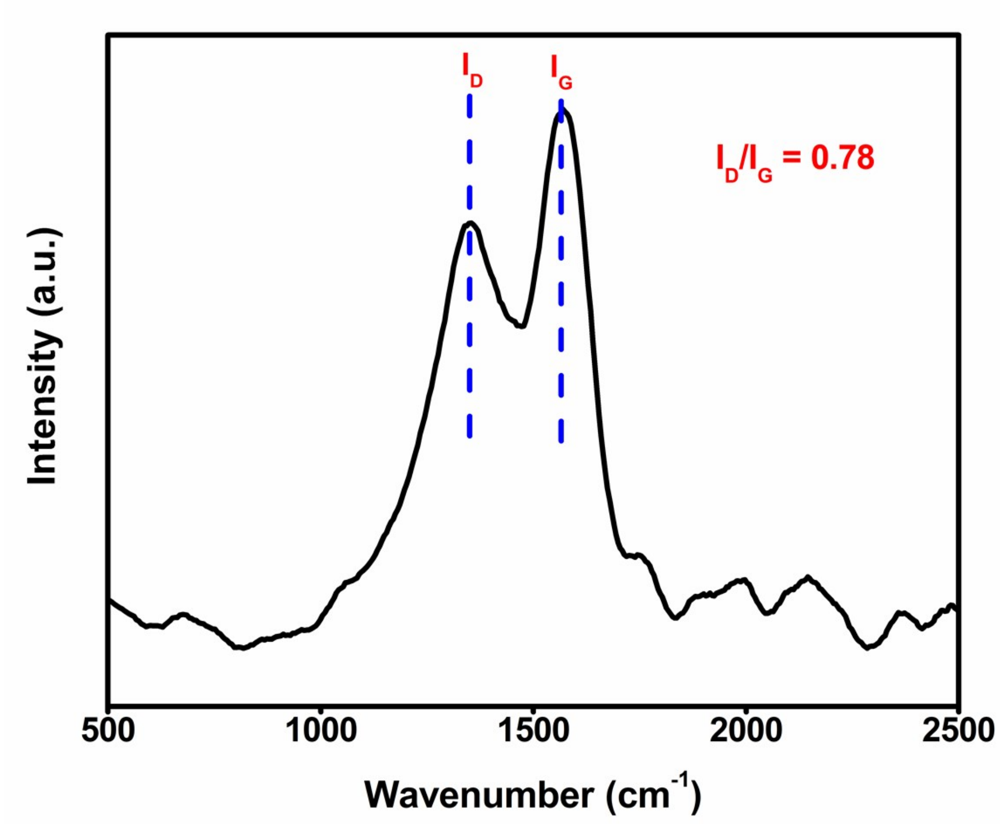

Figure S2. RAMAN spectrum of the prepared Graphene Quantum Dots (GQDs).

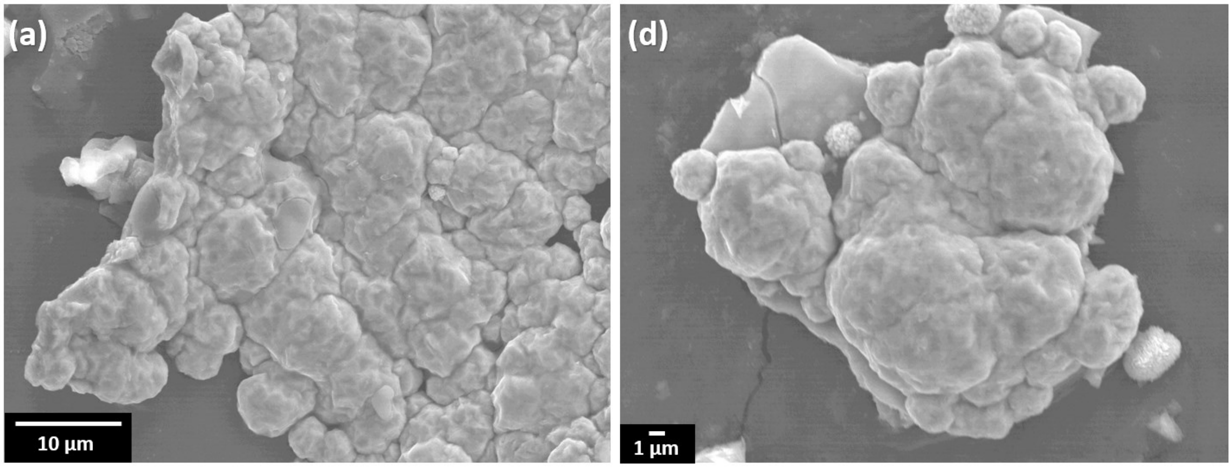

Figure S3. FESEM micrograph of agglomerated GQDs.

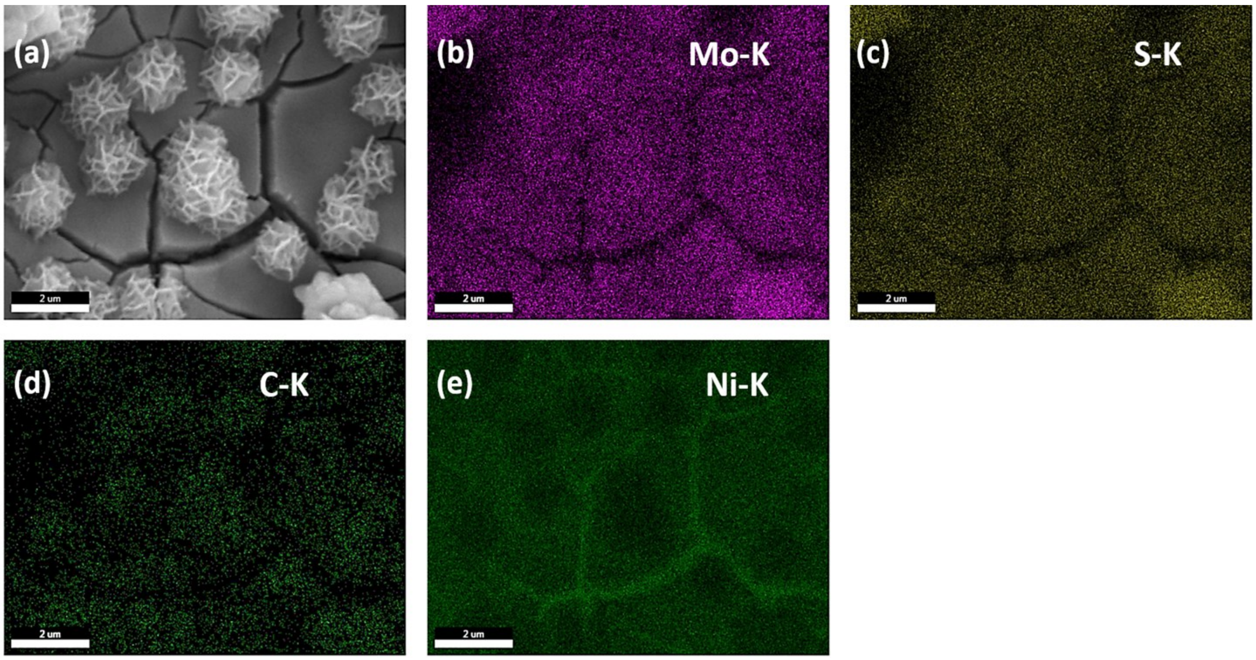

Figure S4. Elemental mapping of MNS-G-2.5 composite.

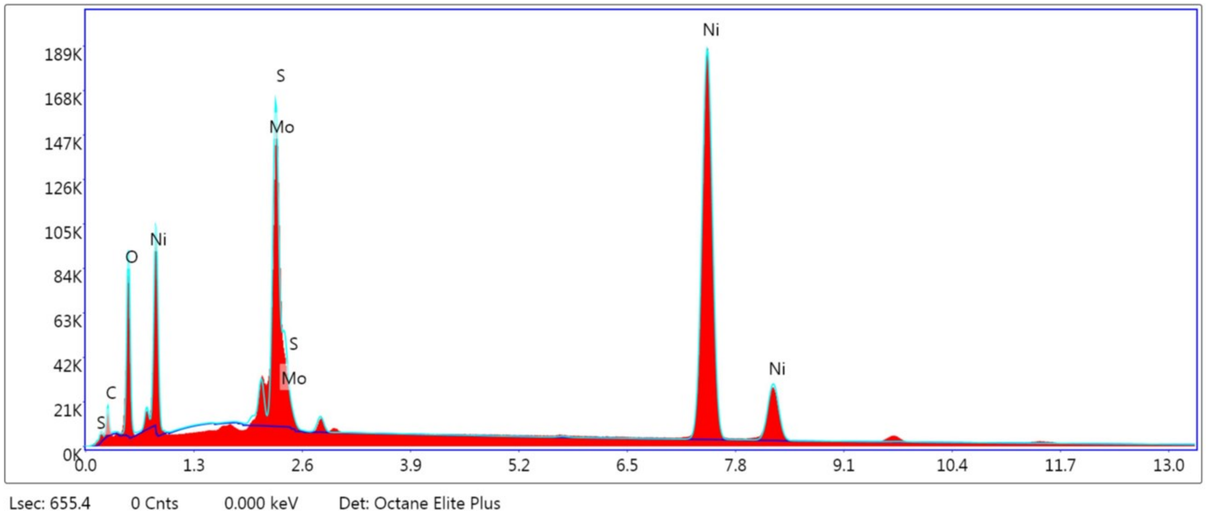

S.No	Element	Weight %
1	C	2
2	Mo	16
3	S	18
4	Ni	55

Figure S5. Energy dispersive spectrum (EDS) of MNS-G-2.5.

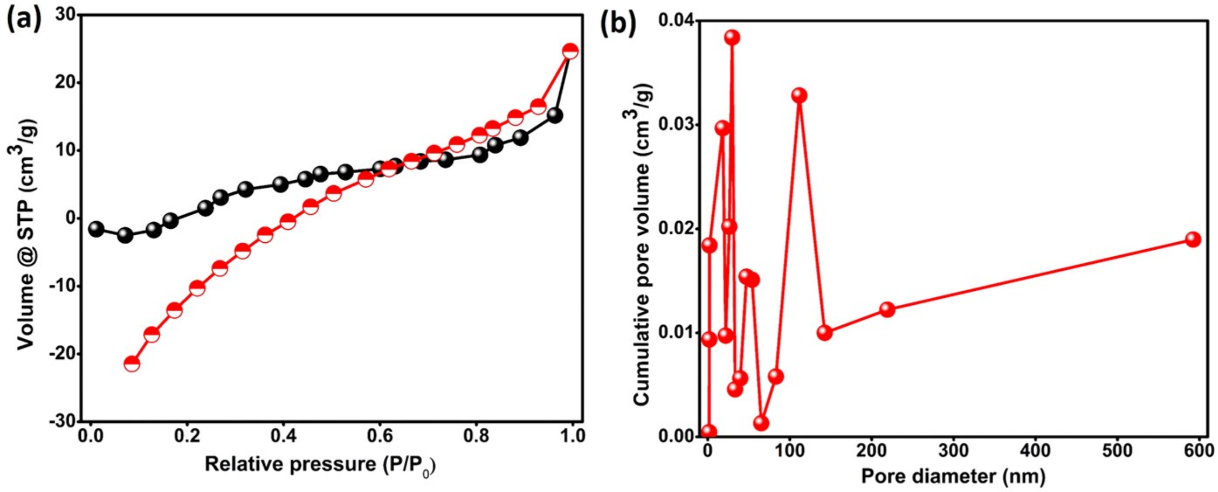

Figure S6. (a) N_2 sorption isotherms for MNS-G-2.5 and (b) Corresponding pore size distribution.

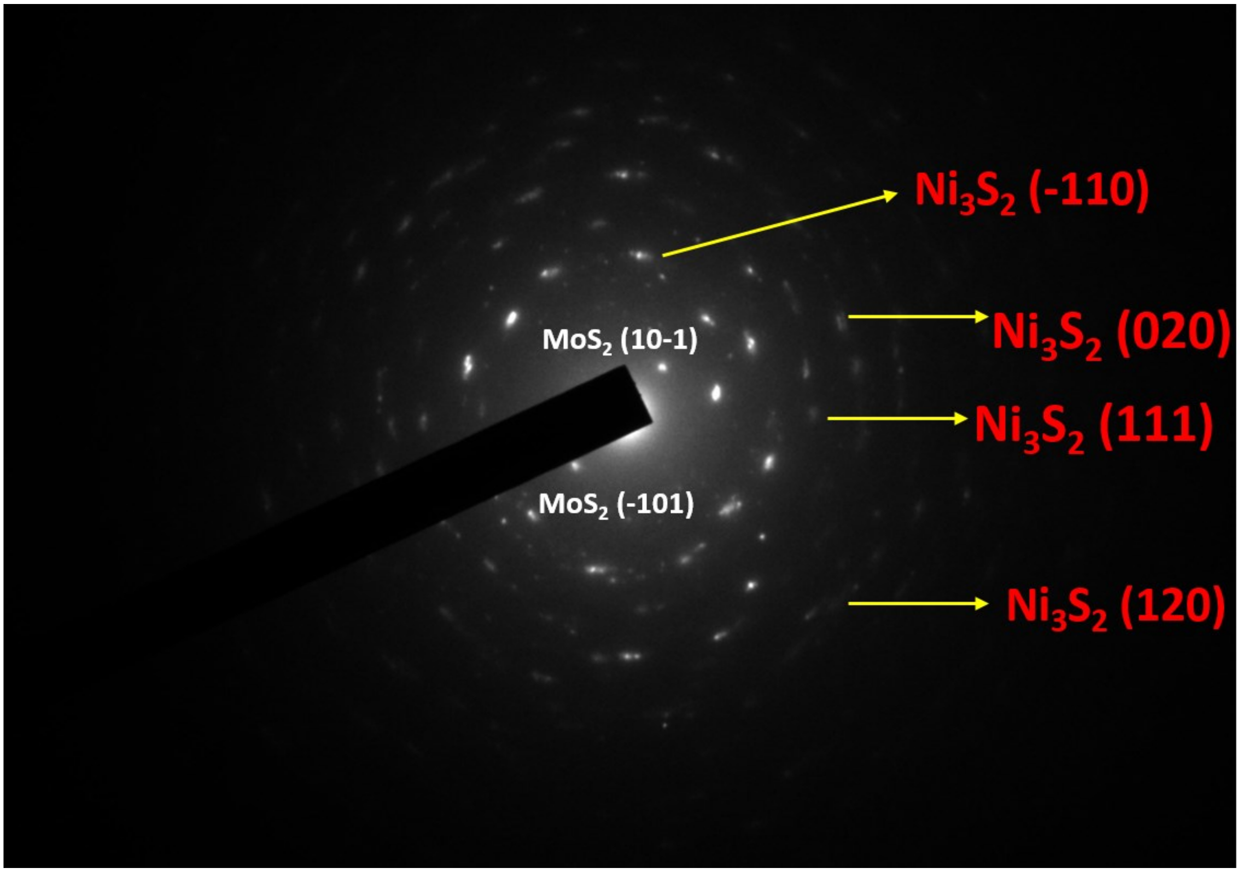

Figure S7. Indexed selected area diffraction (SAED) pattern of MNS-G-2.5 composite.

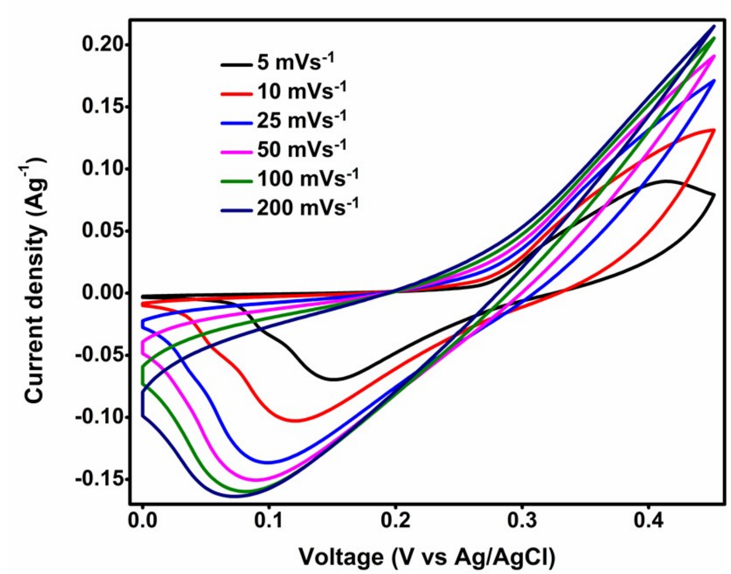

Figure S8. Cyclic Voltammogram (CV) of MNS at different scan rates.

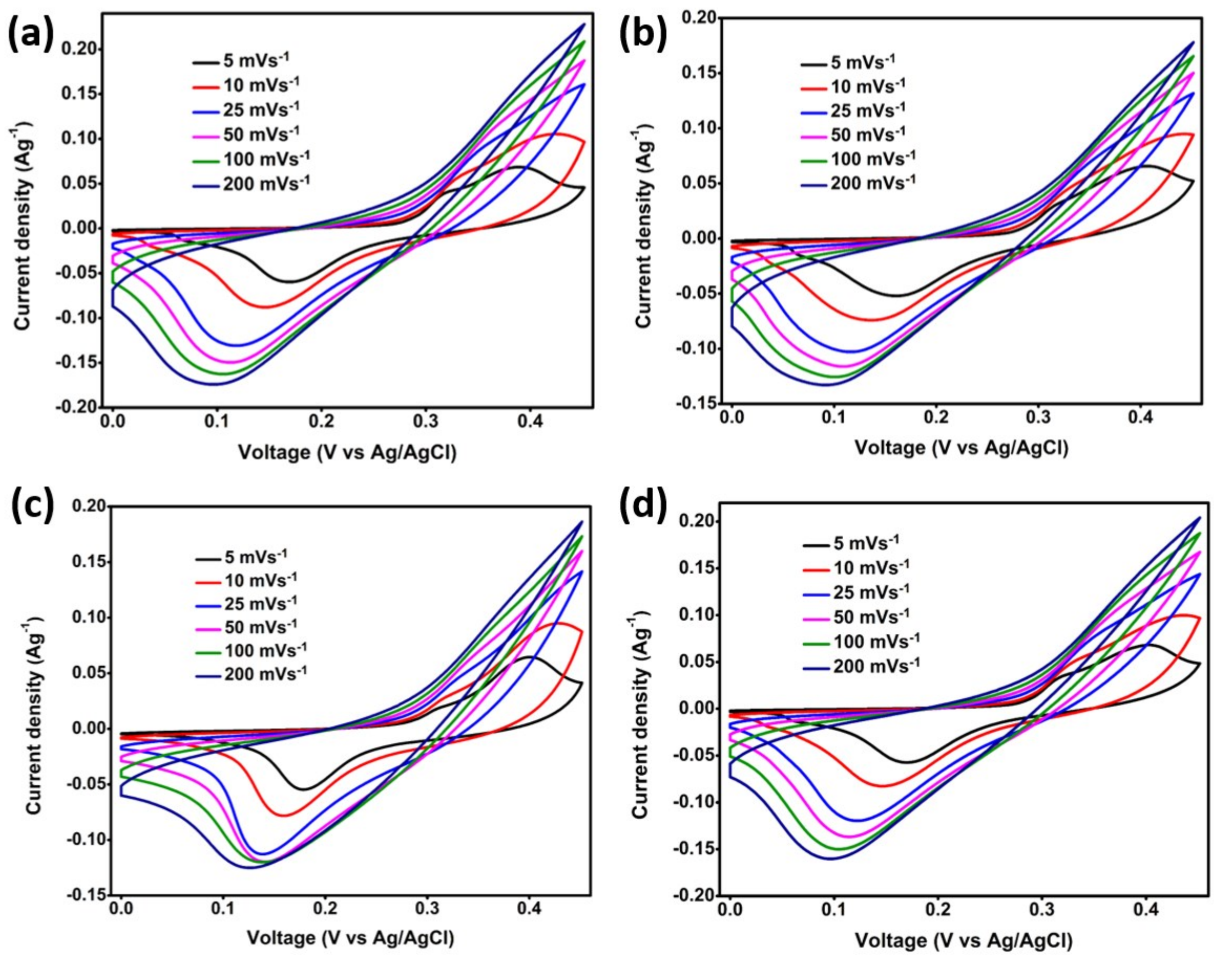

Figure S9. Cyclic Voltammogram (CV) curves of MNS-G-n samples at different scan rates (a) MNS-G-1, (b) MNS-G-2, (c) MNS-G-5 and (d) MNS-G-10.

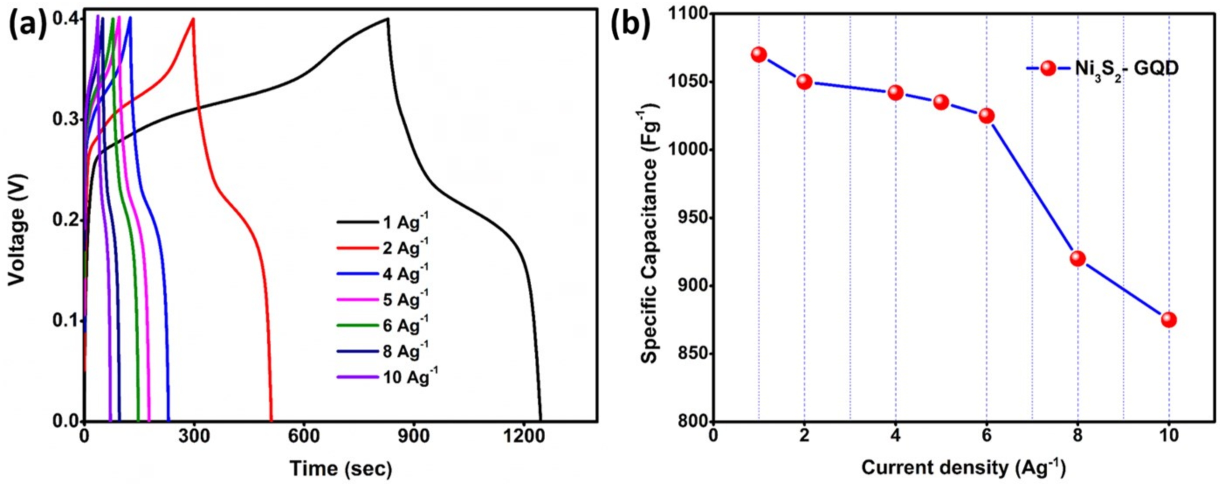

Figure S10. (a) Galvanostatic charge discharge (GCD) curve of Ni_3S_2-GQDs composite at different current densities (b) The mass specific capacitance at different current densities.

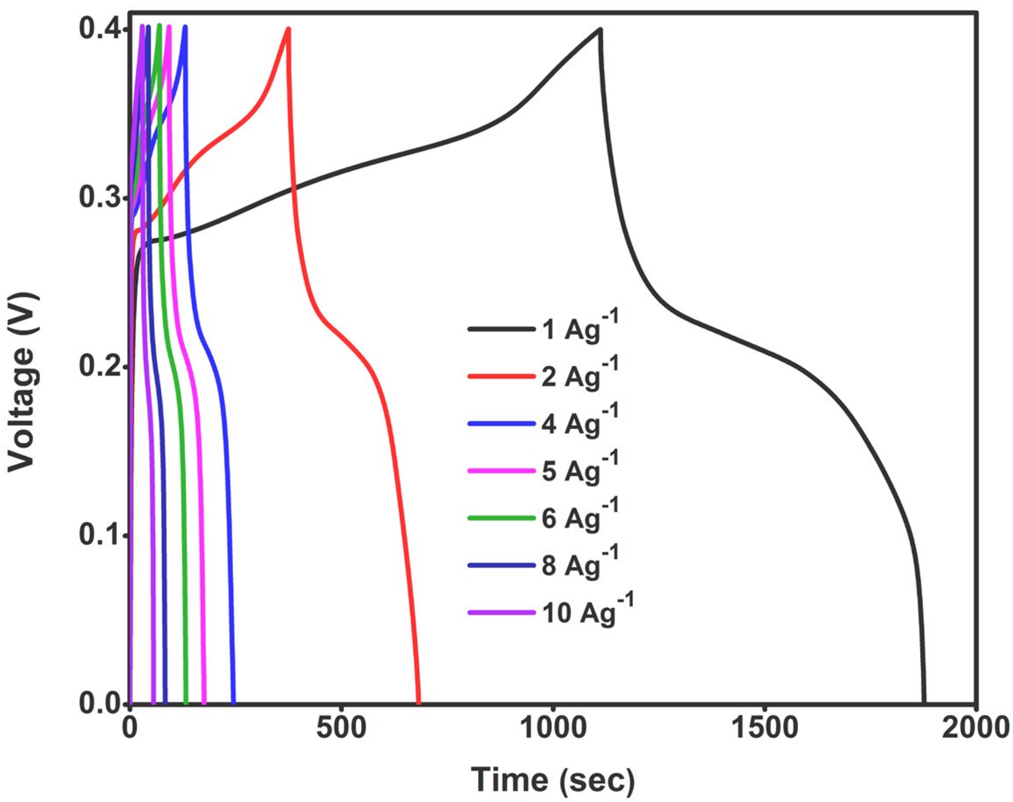

Figure S11. Galvanostatic charge discharge (GCD) curve of MNS at different current densities.

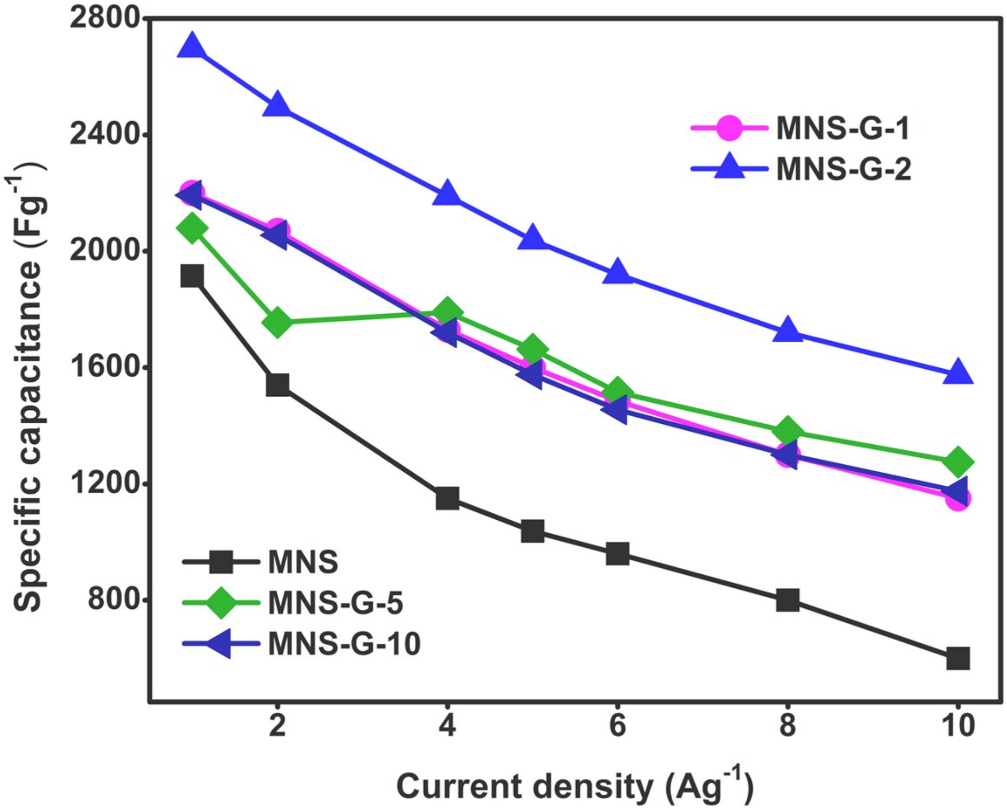

Figure S12. Mass specific capacitance of MNS-G-n composites at different current densities.

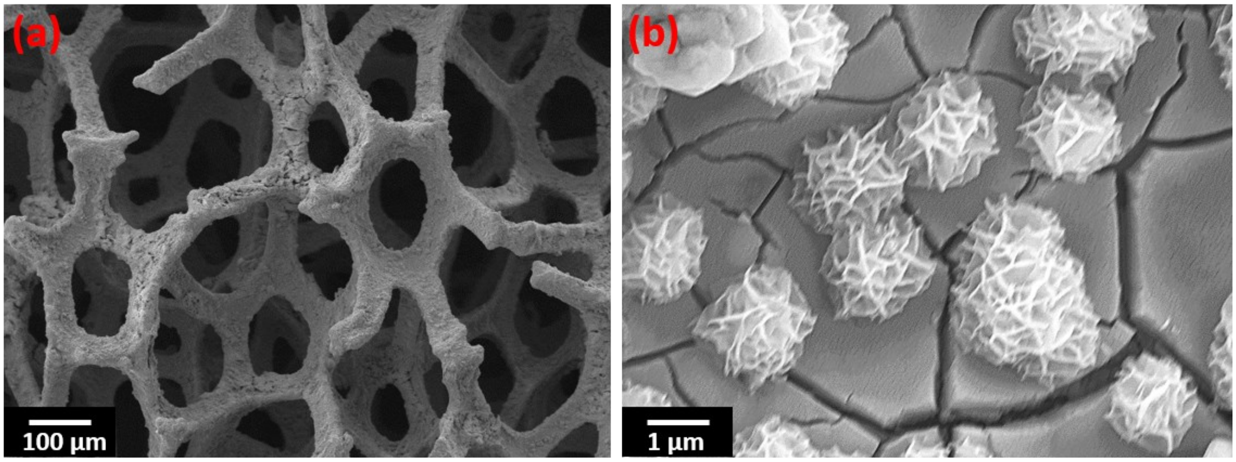

Figure S13. FESEM micrograph of MNS-G-2.5 composite after stability test.

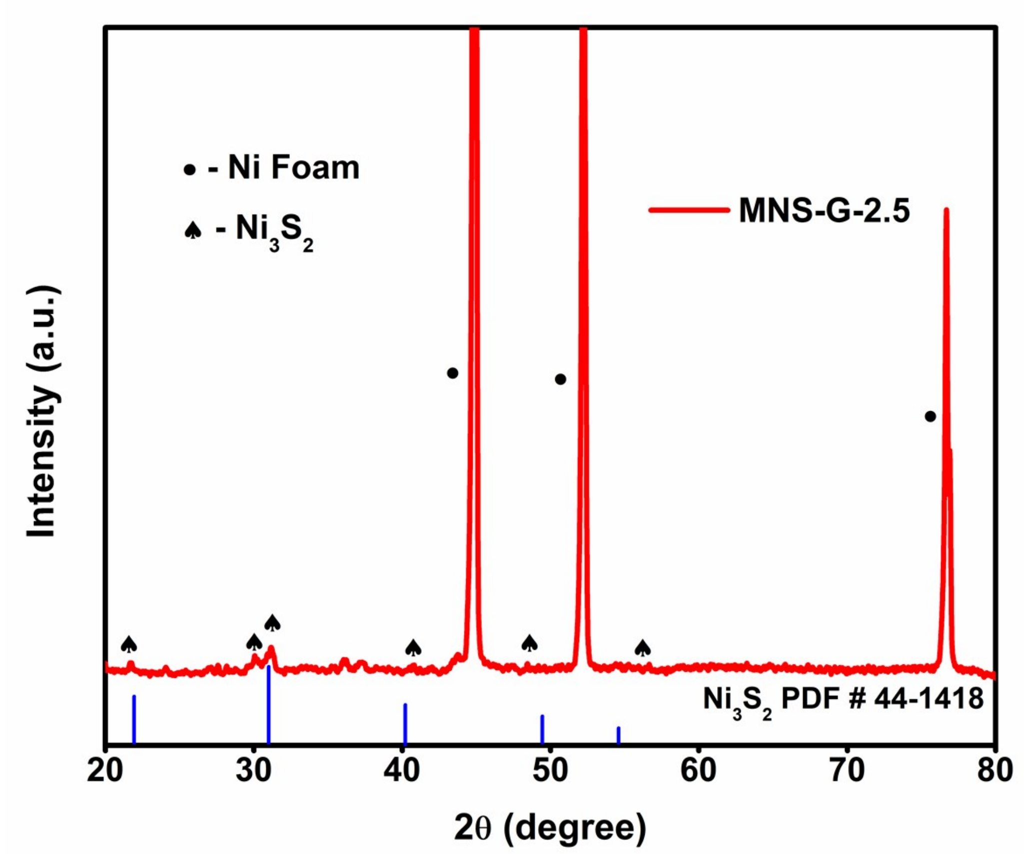

Figure S14. XRD analysis of MNS-G-2.5 composite after stability test.

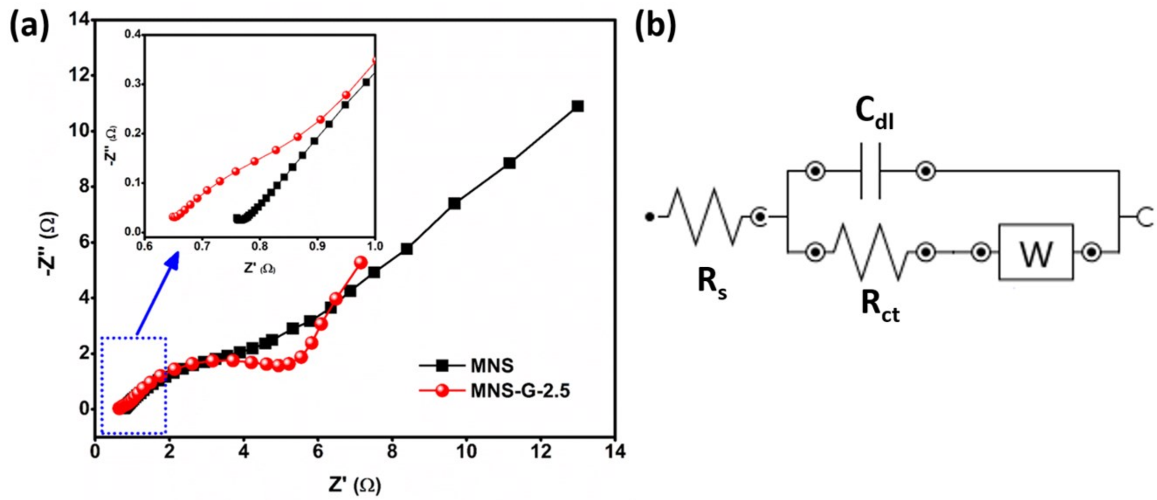

Figure S15. (a) EIS profile of MNS and MNS-G-2.5 composites in the frequency range of 0.01 Hz–100 kHz (b) Corresponding equivalent circuit used for EIS fitting.

Table S1. Performance comparison of the nickel sulfide-based electrode materials in three-electrode configuration with previously published results.

Electrode material	Capacitance	Current density	Cyclic stability	Ref
Ni_3S_2@RGO	2188.8 Fg^{-1}	2.9 Ag^{-1}	90.98 % after 1000 cycles @ 50 mA cm^{-2}	1
NiS	1636.4 Fg^{-1}	2 Ag^{-1}	102.8 % after 1000 cycles @ 50 mVs^{-1}	2
NiS_2/NiO	2251 Fg^{-1}	1 Ag^{-1}	78 % after 2000 cycles @ 5 Ag^{-1}	3
Ni_xS_y@CoS	2291 Fg^{-1}	2 Ag^{-1}	37.6 % after 2000 cycles @ 20 Ag^{-1}	4
$Ni_{0.31}Co_{0.69}S_2$ /graphene	1166 Fg^{-1}	1 Ag^{-1}	74.5 % after 1000 cycles @ 5 Ag^{-1}	5
Ni_7S_6 hollow spheres	2283.2 Fg^{-1}	1 Ag^{-1}	97.1 % after 1000 cycles	6
rGO/Ni_3S_2/Co_9S_8 composite	1929.1 Fg^{-1}	1 Ag^{-1}	86.5% after 1000 cycles @ 20 Ag^{-1}	7
NiS/Ni_3S_4 nanosheets	2070 Fg^{-1}	2.5 Ag^{-1}	86% after 10000 cycles @ 3 Ag^{-1}	8
Rose like Ni_3S_4	1797.5 Fg^{-1}	0.5 Ag^{-1}	----	9
Mushroom like Ni_3S_2	1670 Fg^{-1}	1 Ag^{-1}	89.6 % after 5000 cycles @ 5 Ag^{-1}	10
Co_3O_4@Ni_3S_2 core/shell nanowire arrays	1710 Fg^{-1}	1 Ag^{-1}	85.3 % after 1000 cycles @ 4 Ag^{-1}	11
$Ni_{0.75}Co_{0.25}S_2$	2142 Fg^{-1}	2 Ag^{-1}	75.3 % after 3000 cycles @ 10 Ag^{-1}	12
Graphene-wrapped nickel sulfide nanoprisms	1337 Fg^{-1}	3 Ag^{-1}	71 % after 2000 cycles @ 5 Ag^{-1}	13
Ni_3S_2@graphene	1420 Fg^{-1}	2 Ag^{-1}	2000 cycles @ 6 Ag^{-1}	14
NS-CNT-1	2014.7 Fg^{-1}	10 Ag^{-1}	70.4 % after	15

			6000 cycles @ 10 Ag^{-1}	
NS-CNT-2	2699 Fg^{-1}	10 Ag^{-1}	68.2 % after 6000 cycles @ 10 Ag^{-1}	15
NS-CNT-3	1747 Fg^{-1}	10 Ag^{-1}	76.4 % after 6000 cycles @ 10 Ag^{-1}	15
3D Flower MoNiS	**1915 Fg^{-1}**	**1 Ag^{-1}**	**----**	**This work**
GQD induced 3D flower MoNiS	**2622 Fg^{-1}**	**1 Ag^{-1}**	**92.2 % after 10000 cycles @ 20 Ag^{-1}**	**This work**

References:

1 Z. Zhang, C. Zhao, S. Min and X. Qian, *Electrochim. Acta*, 2014, **144**, 100–110.

2 Z. Li, A. Gu, J. Sun and Q. Zhou, *New J. Chem.*, 2016, **40**, 1663–1670.

3 D. Zhang, X. Zhou, K. Ye, Y. Li, C. Song, K. Cheng, D. Cao, G. Wang and Q. Li, *Electrochim. Acta*, 2015, **173**, 209–214.

4 R. Gao, Q. Zhang, F. Soyekwo, C. Lin, R. Lv, Y. Qu, M. Chen, A. Zhu and Q. Liu, *Electrochim. Acta*, 2017, **237**, 94–101.

5 G. Li and C. Xu, *Carbon N. Y.*, 2015, **90**, 44–52.

6 Z. Li, J. Han, L. Fan and R. Guo, *CrystEngComm*, 2015, **17**, 1952–1958.

7 Y. Chang, Y. Sui, J. Qi, L. Jiang, Y. He, F. Wei, Q. Meng and Y. Jin, *Electrochim. Acta*, 2017, **226**, 69–78.

8 Y. Li, J. Xu, H. Liu, Y. Liu, M. Wang, J. Li and H. Cui, *J. Sol-Gel Sci. Technol.*, 2018, **87**, 546–553.

9 H. Wang, M. Liang, D. Duan, W. Shi, Y. Song and Z. Sun, *Chem. Eng. J.*, 2018, **350**, 523–533.

10 B. Yang, L. Yu, Q. Liu, J. Liu, W. Yang, H. Zhang, F. Wang, S. Hu, Y. Yuan and J. Wang, *CrystEngComm*, 2015, **17**, 4495–4501.

11 J. Zhang, J. Lin, J. Wu, R. Xu, M. Lai, C. Gong, X. Chen and P. Zhou, *Electrochim. Acta*, 2016, **207**, 87–96.

12 S. Xie, J. Gou, B. Liu and C. Liu, *Inorg. Chem. Front.*, 2018, **5**, 1218–1225.

13 A. A. AbdelHamid, X. Yang, J. Yang, X. Chen and J. Y. Ying, *Nano Energy*, 2016, **26**, 425–437.

14 Z. Zhang, X. Liu, X. Qi, Z. Huang, L. Ren and J. Zhong, *RSC Adv.*, 2014, **4**, 37278–37283.

15 P. Lu, X. Wang, L. Wen, X. Jiang, W. Guo, L. Wang, X. Yan, F. Hou, J. Liang, H. M. Cheng and S. X. Dou, *Small*, 2019, **15**, 1–9.